Low-Frequency Spectra of the Wall Shear Stress and Wall Pressure in a Turbulent Boundary Layer

William L. Keith*
Naval Underwater Systems Center, New London, Connecticut 06320
and
John C. Bennett Jr.†
University of Connecticut, Storrs, Connecticut 06269

Measurements of the autospectra of the fluctuating wall shear stress and wall pressure in a fully developed turbulent boundary layer at Reynolds numbers R_Θ = 8200 and 13,400 are presented. The measurements were made in the Quiet Water Tunnel at the Naval Underwater Systems Center. Use of this facility enabled a direct comparison of the spectral levels of both quantities to be made at low frequencies. The frequency ranges over which the pressure and shear stress spectra are accurately resolved are discussed. For these frequencies, the spectra compare favorably with published results at comparable Reynolds numbers. The method used to calibrate the hot-film wall shear stress transducers, based upon the measured mean velocity profiles, is presented in detail. This technique is believed to be the most accurate for high-Reynolds-number turbulent boundary layers of the type investigated here. The error involved in the determination of the mean wall shear stress is shown to be the limiting factor in determining the absolute spectral levels of the fluctuating wall shear stress.

Nomenclature

d	= pressure transducer diameter
E	= anemometer time-varying output voltage
$\bar{E}$	= anemometer mean output voltage
f	= cyclic frequency, cycles/s
L	= hot-film streamwise length, in.
Pr	= Prandtl number
p_{rms}	= wall pressure root mean square
R_Θ	= $U_\infty \Theta/\nu$ = Reynolds number
U_∞	= freestream velocity, ft/s
$u(y)$	= streamwise velocity, ft/s
u_τ	= friction velocity, ft/s
W	= hot-film spanwise width, in.
δ	= boundary-layer thickness, in.
δ^*	= displacement thickness, in.
Θ	= momentum thickness, in.
ν	= kinematic viscosity, ft^2/s
ρ	= fluid density, lbf-s^2/ft^4
τ	= time-varying wall stress, psi
$\bar{\tau}$	= mean wall shear stress, psi
τ_{rms}	= wall shear stress root mean square
$\Phi(\omega)$	= power spectra, psi^2/(rad/s)
ω	= radian frequency, rad/s

Introduction

THIS investigation was aimed at determining the spectral levels at low frequencies of both the fluctuating wall pressure and fluctuating wall shear stress in a fully developed hydrodynamic turbulent boundary layer. The Reynolds numbers investigated were R_Θ = 8,200 and 13,400, corresponding to freestream velocities of 10 and 20 ft/s, respectively. The low-frequency portion of the spectra of these turbulent fluctuations, corresponding to convected wave numbers of the order $2\pi/\delta$, constitutes a primary source of flow-induced noise in many hydrodynamic systems.

Few investigations of turbulent wall shear stress have been reported to date. Recently, Alfredsson et al.[1] discussed measurement techniques and compared various investigations of the turbulent wall shear. They concluded that standard flush-mounted hot-film probes have negligible heat loss to the substrate for water applications, permitting a calibration based on the steady-state heat transfer from the transducers to the fluid. A comparison of the ratio $\tau_{rms}/\bar{\tau}$ obtained in various investigations was presented, but no spectral measurements were discussed. The wide variation of $\tau_{rms}/\bar{\tau}$ between investigations was attributed to such factors as spatial averaging, thermal response, and calibration methods. Madavan et al.[2] made turbulent wall shear spectral measurements with flush-mounted hot films in water at Reynolds numbers comparable to those of this investigation.

Considerably more measurements of the fluctuating wall pressure field have appeared over the past 25 years. Willmarth and Wooldridge [3] presented pressure spectra measured in air at comparable Reynolds numbers using probes similar to those of this investigation. Analogous to the case of the wall shear, a significant variation in the ratio $p_{rms}/\bar{\tau}$ exists between various investigations, due to acoustic contamination occurring at low frequencies and also to spatial averaging occurring at high frequencies.

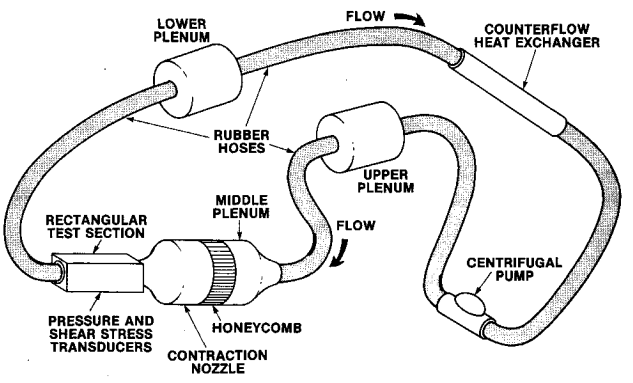

Fig. 1 Quiet water tunnel flow schematic.

Received Aug. 21, 1989; revision received May 9, 1990; accepted for publication June 1, 1990. This paper is declared a work of the U.S. Government and is not subject to copyright protection in the United States.

*Mechanical Engineer, Submarine Sonar Department. Member AIAA.

†Associate Professor, Mechanical Engineering Department. Member AIAA.

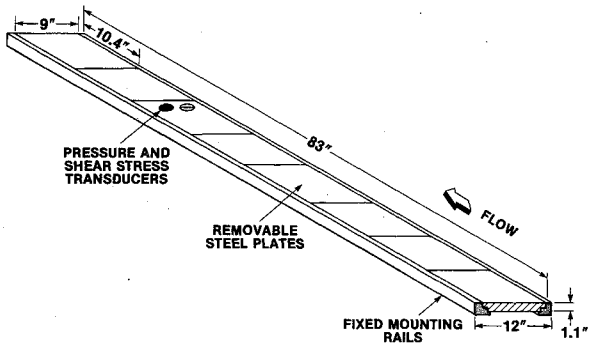

Fig. 2 Transducer mounting on the rectangular test section bottom wall.

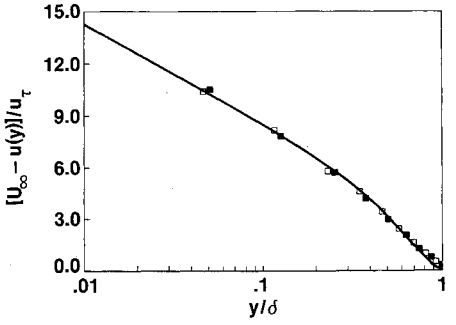

Fig. 3 Velocity defect [■: U_∞ = 10 ft/s; □: U_∞ = 20 ft/s; and —: Eq. (1)].

Experimental Facility and Instrumentation

The experiments were conducted in the rectangular test section of the Quiet Water Tunnel Facility at the Naval Underwater Systems Center New London Laboratory. The water tunnel is a recirculating flow facility, with acoustic isolation provided by rubber hoses between the test section, plenum chambers, and centrifugal pump, as shown in Fig. 1. The temperature of the water was controlled at 72°F with a counterflow heat exchanger. The rectangular test section is 83 in. long, 12 in. wide, and increases in height linearly from 4 in. at the inlet to 4.41 in. at the exit, resulting in a zero pressure gradient flow to within 0.005 psi. The bottom wall of the test section consists of eight removable stainless-steel plates, as shown in Fig. 2. Adjacent plates are positioned flush to within 0.001 in.

The flow converges from the 30-in.-diam middle plenum chamber into the rectangular test section through a contraction nozzle designed to minimize the generation of vorticity. Reduction of the vorticity convected into the test section leads to lower freestream turbulence intensity and reduced spanwise variation in the mean streamwise velocity within the turbulent boundary layer. The freestream turbulence intensity was approximately 1% and the mean streamwise velocity in the boundary layer varied in the spanwise direction by less than ±2%. The boundary-layer parameters determined from the measured mean velocity profiles at the two Reynolds numbers investigated are given in Table 1.

Measurements of the mean and fluctuating streamwise velocities were made with a TSI Model 9100 laser Doppler velocimetry system, operated in the backscatter mode. The measurement volume for these tests was an ellipsoid 0.006 in. in diameter and 0.12 in. long. The major axis of the ellipsoid was oriented in the spanwise direction. The measurement location was controlled by a three-axis TSI traverse system. The uncertainty in the measurement volume location was of the order of the dimensions of the measurement volume. To provide an adequate data rate, a small quantity of silicon-carbide particles was injected into the tunnel, and allowed to mix uniformly prior to any data acquisition. Data analysis was accomplished using a TSI Model 1900 counterprocessor, microcomputer, and modified TSI software. The statistical uncertainty (for a 99% confidence level) was 1% for the mean velocity results at each location.

The pressure and hot-film transducers were flush mounted on the bottom wall of the test section, as shown in Fig. 2. The results presented in this paper are from pressure and shear-stress transducers at the same fixed axial location, approximately 65δ from the test section inlet.

Table 1 Boundary-layer parameters

U_∞, fps	δ, in.	δ*, in.	Θ, in.	R_Θ
10	0.93	0.13	0.10	8200
20	0.74	0.09	0.08	13400

The pressure transducers used were end-capped air-filled cylinders, fabricated of PZT-5H Type 2 material with sensing diameter d of 0.08 in. The transducers were calibrated in air and shown to have a flat response over the frequencies measured in this investigation. The output voltage signals from the transducers were amplified 20 dB by Ithaco Model 143N low-noise preamplifiers, and an additional 20 dB by Ithaco Model 455 amplifiers with adjustable high-pass filters (set at 1 Hz). The signals were then processed with a Spectral Dynamics Model SD375 spectrum analyzer with 400 lines of spectral resolution. The absolute pressure spectra measured from the various transducers, and converted using the respective calibration constants, were found to agree to within ±1/2 dB at all frequencies.

The hot-film shear-stress transducers used were TSI Model 1268W with a streamwise length L of 0.005 in. and a spanwise width W of 0.04 in. The transducers were operated at an overheat ratio of 1.07 and controlled in the constant-temperature mode with a TSI Model IFA100 anemometry system. No signal conditioning was performed prior to processing the data with either the spectrum analyzer or HP3456A digital voltmeter. The rms voltages measured using the digital voltmeter agreed extremely well with the values calculated by integrating the voltage spectra numerically.

Hot-Film Transducer Calibration

The velocity profiles measured normal to the bottom plate were used to evaluate the quality of the turbulent boundary layer and also to calibrate the hot-film transducers. Coles' empirical formula[4] for the velocity defect is

$$[U_\infty - u(y)]/u_\tau = -2.5 \ln [y/\delta] + 1.38 [2 - w_c(y/\delta)] \quad (1)$$

where $w_c(y/\delta)$ is the wake function. Equation (1) includes both the boundary thickness δ and the friction velocity u_τ as scaling parameters. The values for δ were determined from the mean velocity profiles such that $u(\delta) = 0.99U_\infty$. The measured values of the mean velocity closest to the wall were then used in conjunction with Eq. (1) to calculate the values for the friction velocity u_τ. The resulting uncertainty in the u_τ values was 2%. The profiles measured at the location of the pressure and hot-film transducers were found to agree well with Eq. (1) as shown in Fig. 3. The ratios u_τ/U_∞ for the two Reynolds numbers, listed in Table 2, are consistent with the results of Coles[5] both in terms of the magnitudes and trend with Reynolds number. Based on these results together with the measured values of R_Θ, a fully developed turbulent boundary layer existed at both Reynolds numbers. Also listed in Table 2 are the transducer dimensions expressed in terms of the inner length scale ν/u_τ. Although the hot-film transducers used are the smallest that are commercially available, the extremely small inner length scales resulted in significant spatial averaging leading to attenuations at the higher frequencies.

To calibrate the hot-film transducers, it was necessary to de-

termine the variation in the mean output voltage with mean wall shear stress at each Reynolds number. Direct measurements of the mean wall shear stress, involving velocity measurements in the viscous sublayer (less than 0.002 in. from the wall), were not possible. Therefore, values for the mean wall shear were calculated from the friction velocities that were determined from the mean velocity profiles. The uncertainty in the values obtained for the mean wall shear was 4%.

The freestream velocity was varied about both the 10- and 20-fps operating points. For each freestream velocity, both the mean velocity profile and transducer mean output voltage were recorded. Using a fourth-order polynomial curve fit to these data, the variation in mean transducer voltage with mean wall shear stress was determined. The resulting calibration curves are shown in Figs. 4 and 5. From these curves, the values for $d\bar{\tau}/d\bar{E}$ were determined. This parameter was then used to convert transducer voltage spectra to wall shear-stress spectra. Since the rms voltage levels were approximately 2% of the mean voltages, this first-order conversion was valid.

Sandborn[6] presents a calibration equation for flush-mounted hot-film transducers, of the form

$$\tau^{1/3} = AE^2 + B \tag{2}$$

where A and B are constants. The calibration data of Figs. 4 and 5 fitted to the form of the mean of Eq. (2) to first-order are shown in Figs. 6 and 7, respectively. These data are in support of the functional form of Eq. (2). Note however that there is a systematic deviation of the data from this relationship. In addition, the constants A and B change as the Reynolds number increases. For these reasons, the previously described calibration procedure provides greater accuracy, particularly as the number of calibration data points increases.

The accuracy in determining the absolute spectral levels for the wall shear stress is limited by the uncertainty in the calibration parameter $d\bar{\tau}/d\bar{E}$. Using the method involving curve fits to the actual data, the scatter in the calculated values of $d\bar{\tau}/d\bar{E}$ leads to an uncertainty of 2 dB for the spectra. This overall uncertainty in the spectral levels is primarily due to the uncertainty in the calculated friction velocity values. In principle, increasing both the number of velocity samples per profile as well as the number of profiles would reduce this uncertainty. In practice, complications arise due to slow variations in the fluid temperature and freestream velocity, which occur over the long time durations needed for such measurements. For boundary layers with sufficiently small inner length scales to preclude velocity measurements within the sublayer, this calibration method is however believed to be the most accurate.

Table 2 Inner scales and transducer dimensions

U_∞, fps	u_τ/U_∞	ν/u_τ, in.	du_τ/ν	Lu_τ/ν	Wu_τ/ν
10	0.035	0.00034	235	15	120
20	0.032	0.00019	420	25	210

Following Bellhouse and Schultz,[7] a steady-state analysis of the heat transfer from the hot film was used to determine the thermal boundary-layer thickness at each Reynolds number. The thermal boundary layer δ_t, was found to be entirely within the viscous sublayer at each Reynolds number, as shown in Table 3. The resulting linear velocity profile throughout the thermal boundary layer permitted an unsteady heat-transfer analysis to be done. The resulting one half power frequency is given by

$$\omega_{1/2} = 2.63\,\nu[Pr(L\nu^2/u_\tau^2)^2]^{-1/3} \tag{3}$$

where Pr is the Prandtl number. The half-power frequencies for each Reynolds number are given in Table 3. Details of the steady and unsteady heat-transfer analyses are given by Keith.[8]

Wall Shear and Pressure Spectra

The wall shear spectra will be presented in both normalized and non-normalized forms. The use of the measured rms voltages to normalize the hot-film voltage spectra allows the shape of the spectra to be compared, independent of the method of

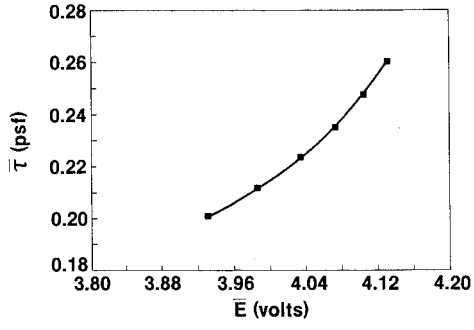

Fig. 4 Hot-film calibration (■: U_∞ = 10 ft/s; and —: $\bar{\tau}$ = 0.231, $\bar{E}^4$ −0.679, $\bar{E}^3$ −13.338, $\bar{E}^2$ +80.911, $\bar{E}$ −125.022).

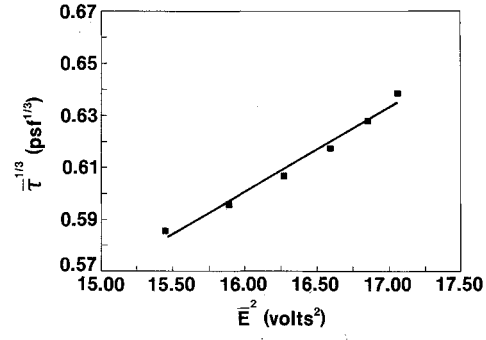

Fig. 6 Hot-film calibration (■: U_∞ = 10 ft/s; and —: $\bar{\tau}^{1/3}$ = 0.032, $\bar{E}^2$ + 0.083).

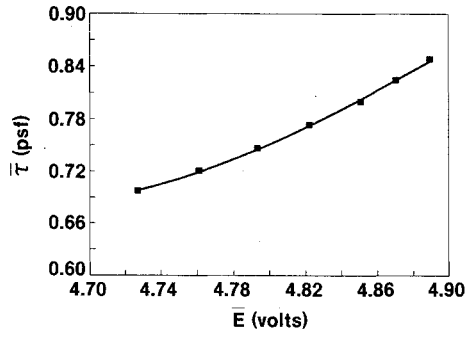

Fig. 5 Hot-film calibration (■: U_∞ = 20 ft/s; and —: $\bar{\tau}$ = 0.104, $\bar{E}^4$ −0.925, $\bar{E}^3$ +29.828, $\bar{E}^2$ −175.379, $\bar{E}$ +312.985).

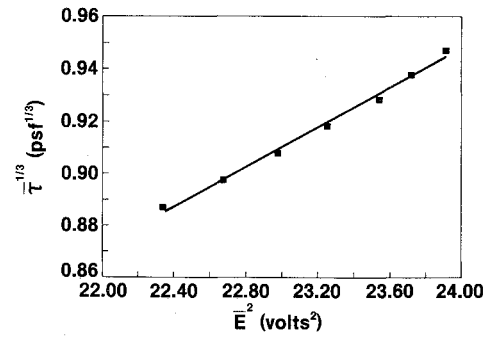

Fig. 7 Hot-film calibration (■: U_∞ = 20 ft/s; and —: $\bar{\tau}^{1/3}$ = 0.038, $\bar{E}^2$ + 0.038).

Table 3 Transducer response parameters

U_∞, fps	$\delta_i u_\tau/\nu$	$f_{1/2}$, Hz	$\omega_{1/2}\delta^*/U_\infty$	$\omega_{1/2}\nu/u_\tau^2$
10	4.65	468	3.18	0.24
20	5.72	1016	2.40	0.16

calibration with its associated errors. These normalized spectra will be presented in two forms, with the frequency variable nondimensionalized on inner and outer scales, respectively. The non-normalized, or absolute spectra, will be presented in two standard nondimensional forms, using inner and outer scales, respectively. This latter form allows a comparison of the absolute spectral levels of both the wall pressure and wall shear.

The normalized wall shear spectra are shown in Figs. 8 and 9, where the frequency variable has been nondimensionalized using inner and outer scales, respectively. It is noted that only a frequency scale is needed in order to nondimensionalize the normalized spectra. The ratio of the inner frequency scale to the outer frequency scale ω_i/ω_o (where $\omega_i = u_\tau^2/\nu$, and $\omega_o = U_\infty/\delta^*$) was 13.4 for $U_\infty = 10$ ft/s, and 15.2 for $U_\infty = 20$ ft/s. For the vertical scaling of the normalized spectra, the effective difference between the inner and outer scaling is therefore ½ dB. For the horizontal scaling, the effective difference is 13%. The uncertainty in the measured normalized spectral levels was within ¼ to ½ dB. The uncertainties for u_τ and δ^* were 2% and 5%, respectively. For these reasons, conclusions as to whether the inner or outer scaling is more effective for collapsing the normalized spectra are not possible. The results presented in Figs. 8 and 9 confirm that both scalings work equally well, as would be expected in view of the previous remarks.

At frequencies where attenuations in the spectral levels due to spatial averaging are occurring, the effectiveness of a particular scaling (either inner or outer) cannot be determined unless corrections are applied. In the case of outer scaling, the wave numbers that contribute energy at a particular nondimensional frequency $\omega\delta^*/U_\infty$ vary inversely with the length scale δ^*. As the Reynolds number increases and δ^* decreases, the contributing wave numbers become larger, and the attenuation due to spatial averaging increases. The same is true for the case of inner scaling.

Results presented by Madavan et al.[2] for a comparable Reynolds number are also shown in Fig. 8. The two sets of normalized spectra compare favorably. A more rapid rolloff at higher frequencies for the Madavan et al.[2] data, as shown in Fig. 8, is likely due to the effects of spatial averaging associated with their somewhat larger transducers.

To compare the absolute spectral levels of the wall shear and wall pressure at each Reynolds number, the voltage spectra must first be converted to common dimensional forms using the appropriate calibration parameters. The absolute spectra of the wall shear scaled on inner variables are presented in Fig. 10. These spectra are compared with the data of Madavan et al.[2] No absolute spectra were presented in Ref. 2. Therefore, in making this comparison, a value of 0.22 for $\tau_{rms}/\bar{\tau}$ was used to convert the normalized spectra presented by the authors. The values reported in Ref. 2 for $\tau_{rms}/\bar{\tau}$ at R_Θ approximately equal to 5600 varied from 0.19 to 0.24. This spread in reported values corresponds to an uncertainty of 1 dB in the absolute spectral levels presented here. The uncertainty associated with the method of calibration in Ref. 2 is unknown.

It seems reasonable, in view of the calibration uncertainty and the excellent agreement between the normalized spectra, that the difference in absolute spectral levels at low frequencies for the three cases shown in Fig. 10 may be attributed to the calibration procedure.

Alfredsson et al.[1] present a comparison of the ratios $\tau_{rms}/\bar{\tau}$ reported by various investigators, using different calibration and acquisition techniques. The tabulated results showed a range in values from 0.06 to 0.40. This wide variation was attributed to such factors as heat loss to the substrate, spatial averaging, and the frequency response of the various transducers. The values measured in the present investigation, 0.17 and 0.13, for freestream velocities of 10 and 20 fps, respectively, fall within this range. The uncertainty in these values associated with the calibration procedure is 25%. Accepting the conclusions in Ref. 1 that no significant heat loss to the substrate occurs for testing in water, these values reflect the attenuations due to spatial averaging and thermal response already noted. A procedure that would correct for these attenuations is necessary to compare the various reported rms values. However, a correction procedure for spatial-averaging effects requires spatial correlation information, which is presently not available. Therefore, the approach taken here was to compare the spectra over the lower frequency ranges (where the associated attenuations are negligible).

The spectra of both the wall shear and wall pressure scaled on outer variables are shown in Fig. 11. The previous discussion concerning inner and outer scaling for the normalized wall shear spectra also applies to the absolute spectra. In particular, the uncertainty of 2 dB associated with the calibration procedure is comparable to the difference at the two Reynolds

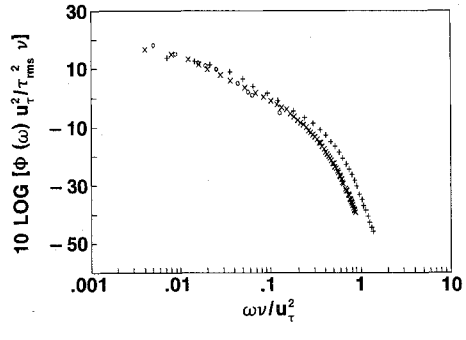

Fig. 8 Normalized wall shear-stress spectra scaled with inner variables (+: $U_\infty = 10$ ft/s; ×: $U_\infty = 20$ ft/s; and ○: Madavan et al.[2]).

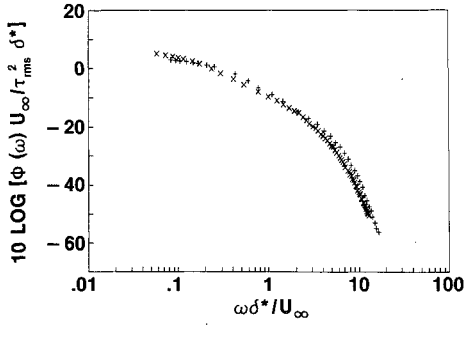

Fig. 9 Normalized wall shear-stress spectra scaled with outer variables (+: $U_\infty = 10$ ft/s; and ×: $U_\infty = 20$ ft/s).

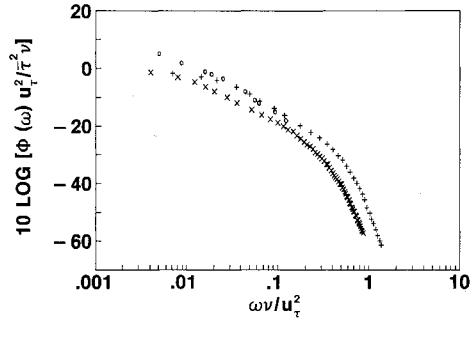

Fig. 10 Absolute wall shear-stress spectra scaled with inner variables (+: $U_\infty = 10$ ft/s; ×: $U_\infty = 20$ ft/s; and ○: Madavan et al.[2]).

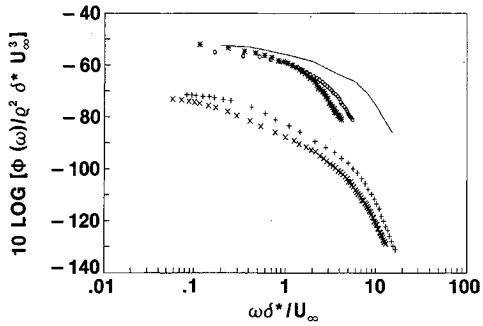

Fig. 11 Absolute spectra scaled with outer variables (+: wall shear stress for U_∞ = 10 ft/s; ×: wall shear stress for U_∞ = 20 ft/s; ○: wall pressure for U_∞ = 10 ft/s; ∗: wall pressure for U_∞ = 20 ft/s; and ——: wall pressure from Willmarth and Wooldridge[3]).

numbers of the ratio of the inner-to-outer scaling of the spectral density.

In view of the dimensions of the pressure transducers used here, as given in Table 2, one would expect the spatial averaging occurring at the higher frequencies to be more severe for the pressure than the wall shear. The effect of spatial averaging on the measurement of wall-pressure spectra has been investigated by Bull and Thomas,[9] Corcos,[10] and Willmarth and Roos.[11] Clearly significant attenuation of the convected wall-pressure field occurred at the higher frequencies here. Blake[12] states that for $\omega d/U_\infty < 1.2$, the effects of spatial averaging are negligible. Corresponding frequencies $\omega\delta^*/U_\infty$ for U_∞ = 10 and 20 fps are 2.0 and 1.4 (or 300 and 600 Hz), respectively. These frequencies determine the upper limit for the range over which an accurate comparison of the spectra of the pressure and wall shear may be made. At nondimensional frequencies below 0.24 and 0.12 (or 35 and 50 Hz) for U_∞ = 10 and 20 fps, respectively, the spectral levels of the pressure fluctuations were influenced by acoustic noise generated by the centrifugal pump and transmitted by the working fluid.

Shown in Fig. 11 are the pressure spectra from the present investigation scaled on outer variables along with the results of Willmarth and Wooldridge[3] made in a thick turbulent boundary layer of air at a comparable Reynolds number. The ratios d/δ^* for the present investigation were 0.62 and 0.89 for U_∞ = 10 and 20 fps, respectively, as compared with 0.36 for Ref. 3. The pressure transducers used here were approximately one half the diameter of those for Ref. 3, and the boundary layer here was approximately one-fifth as thick. Spatial averaging therefore accounts for the more rapid rolloff at the higher frequencies in this investigation. Note that this rolloff is slightly greater for the higher Reynolds number in this investigation, consistent with both the Blake rolloff criteria discussed earlier and also with the previous argument regarding the relationship between wave numbers and Reynolds number. For the lower frequencies over which the pressure spectra here are accurately resolved, the outer variable scaling results in a collapse of the data from this investigation and Ref. 3. This comparison also shows that contributions to the respective spectra from acoustic noise were negligible.

The spectral levels of the wall shear vary from approximately 18 to 24 dB below that of the wall pressure, at the lower frequencies, for both Reynolds numbers investigated here. Although these results hold for a limited range of Reynolds numbers, they provide a direct comparison of spectral levels pertinent for the modeling of flow induced noise and vibration.

Conclusions

For the results of this investigation, the spectral levels of the wall pressure and wall shear were accurately resolved at low frequencies. The spectra agree well with other investigations for frequencies where attenuations due to various sources are not significant. The accuracy of the absolute spectra is limited by the uncertainty associated with the calibration of the hot-film transducers for wall shear-stress measurements. The calibration method presented here involves the use of a well-established empirical formula for boundary-layer profiles to determine the local mean wall shear stress. This estimate of the local mean wall shear stress is believed to be more direct and more accurate than other contemporary methods. As a consequence, the resulting uncertainties in the calibration parameters and absolute spectral levels are reduced.

Further measurements of the spatial correlation of the fluctuating wall shear stress are necessary to fully characterize the field, and determine more details involving the relationship to the wall pressure. As hot-film transducers are not subject to contamination from acoustic waves in the working fluid, it is conceivable that they may be of use as an indirect indicator of contributions to the wall-pressure spectra from convected turbulence corresponding to very low frequencies.

Acknowledgments

The authors are grateful to W. Willmarth at the University of Michigan together with H. Bakewell and W. Strawderman at the Naval Underwater Systems Center (NUSC) for many helpful discussions. D. Hamilton and J. Barclay assisted in the data acquisition and analysis. Funding for W. Keith was provided by the Office of Naval Research, Code 1125, and the NUSC IR/IED Program. Funding for J. Bennett was provided through the Navy-ASEE Summer Faculty Research Program. The authors are also grateful to W. VonWinkle of NUSC for his support.

References

[1]Alfredsson, P. H., Johansson, A. V., Haritonidis, J. H., and Eckelman, H., "The Fluctuating Wall-Shear Stress and the Velocity Field in the Viscous Sublayer," *Physics of Fluids,* Vol. 31, No. 5, 1988, pp. 1026–1033.

[2]Madavan, N. K., Deutsch, S., and Merkle, C. L., "Measurements of Local Skin Friction in a Microbubble- Modified Turbulent Boundary Layer," *Journal of Fluid Mechanics*, Vol. 156, 1985, pp. 237–256.

[3]Willmarth, W. W., and Wooldridge, C. E., "Measurements of the Fluctuating Pressure at the Wall Beneath a Thick Turbulent Boundary Layer," *Journal of Fluid Mechanics*, Vol. 14, Pt. 2, 1962, pp. 187–210.

[4]Coles, D., "The Law of the Wake in the Turbulent Boundary Layer," *Journal of Fluid Mechanics*, Vol. 1, 1956, pp. 191–226.

[5]Coles, D., "Measurements in the Boundary Layer on a Smooth Flat Plate in Supersonic Flow—Pt. 1: The Problem of the Turbulent Boundary Layer," Jet Propulsion Lab., California Inst. of Technology, Pasadena, CA, Rept. 20-69, 1953.

[6]Sandborn, V. A., *Resistance Temperature Transducers,* Metrology, Fort Collins, CO, 1972, pp. 377–382.

[7]Bellhouse, B. J., and Schultz, D. L., "The Measurement of Fluctuating Skin Friction in Air with Heated Film Gauges," *Journal of Fluid Mechanics*, Vol. 32, 1968, pp. 675–680.

[8]Keith, W. L., "Spectral Measurements of the Wall Shear Stress and Wall Pressure in a Turbulent Boundary Layer—Part I: Theory," Naval Underwater Systems Center, New London, CT, TR-8295, 1989.

[9]Bull, M. K. and Thomas, S. W., "High-Frequency Wall Pressure Fluctuations in Turbulent Boundary Layers," *Physics of Fluids,* Vol. 19, No. 4, 1976, pp. 597–599.

[10]Corcos, G. M., "Resolution of Pressure in Turbulence," *Journal of the Acoustical Society of America*, Vol. 35, No. 2, 1962, pp. 192–199.

[11]Willmarth, W. W., and Roos, F. W., "Resolution and Structure of the Wall Pressure Field Beneath a Turbulent Boundary Layer," *Journal of Fluid Mechanics,* Vol. 22, 1965, pp. 81–94.

[12]Blake, W. K., *Aero/Hydroacoustics for Ships,* Vol. 2, DTNSRDC-84/010, David Taylor Research Center, Bethesda, MD, 1984, pp. 729–736.